Total and Double Differential Scattering Cross-Section Measurements of Isotropic Graphite

Atsushi Kimura[1*], *Shunsuke* Endo[1], and *Shoji* Nakamura[1]

[1] Japan Atomic Energy Agency, 2-4 Shirakata, Tokai, Ibaraki, Japan

Abstract. The total and double differential scattering cross sections (DDSCS) of isotropic graphite have been measured in the J-PARC Materials and Life Science Experimental Facility using five samples with different porosities and grain sizes. The DDSCS measurements were performed in Beam Line No.14 (AMATERAS) with nine incident neutron energies ranging from 1.2 to 94 meV. In the derived cross sections, there are no clear sample dependence. The neutron total cross sections in the energy region from 1 to 100 meV were measured using Beam Line No. 04 (ANNRI). All samples in the epithermal range (over 40 meV) tended to have values close to the free atom cross-section of graphite. However, at the first Bragg edge, the deduced total cross sections by these measurements started to vary. The difference became more significant with decreasing the neutron energy.

1 Introduction

Graphite has been considered an efficient neutron moderator and reflector because of its small atomic mass number, small neutron capture cross section, large scattering cross section, easy availability, and comparatively low cost. To deduce the neutron spectrum, it is imperative to obtain precise cross-section data of graphite in the low energy range [1]. However, the cross sections are influenced by the thermal neutron scattering law depending on the crystal structure, and the reported results have significant discrepancies [2]. In order to examine the origin of these discrepancies, the total and double differential scattering cross sections (DDSCS) of isotropic graphite were measured at the Materials and Life Science Experimental Facility (MLF) at J-PARC.

2 Samples

Isotropic graphite is a graphite that is isotropically formed with cold isostatic pressing (CIP). In the CIP, the raw material is filled into a rubber mold, placed in a pressure vessel filled with water or oil, and compresses the material under high pressure [3]. As a result, isotropic graphite has high density, high strength, high thermal conductivity, and uniform characteristics in three dimensions. Isotropic graphite is widely used for general industrial

* Corresponding author: kimura.atsushi04@jaea.go.jp

components. Using these excellent properties, isotropic graphite is used in the Japanese high-temperature gas reactor, HTTR, as fuel assembly and reflectors [4].

Five isotropic graphite samples with different densities, porosities, and grain sizes were used as samples in the experiments. The samples are cylindrical with a diameter of 10mm and a height of 10mm and supplied by Ibiden Co. Ltd. Table 1 shows the typical properties of the sample materials. ET-10, -11, and 34 are graphite for general industrial purposes with different porosities. ED-4 is a sample with a very small grain size used in Electrical Discharge Machining (EDM). T-8 is a high-purity (less than 5 ppm) graphite used in ion implanters. The other samples have impurities of less than 100 ppm.

Table 1 Typical properties of the isotropic graphite samples.

Type	Density (g/cm^3)	Porosity (%)	Grain Size (μm)	Place of Use
ET-10	1.75 (1.75)*	15*	15*	Graphite for general purposes: Industrial furnaces and reactors (Made with a similar process)
ET-11	1.76 (1.77)*	14*	13*	
ET-34	1.84 (1.86)*	11*	15*	
ED-4	1.90 (1.90)*	9*	1*	Graphite for EDM
T-8	1.88 (1.85)*	9*	5*	Graphite for ion implanters (High purity < 5ppm)

*: Typical (nominal) value

3 Double differential scattering cross-section measurement

3.1 Experimental setup

DDSCS measurements were performed in beamline No. 14, named Cold-Neutron Disk-Chopper Spectrometer (AMATERAS). The AMATERAS spectrometer is a disk-chopper-type instrument. Neutrons are monochromatised using the disk choppers. The monochromatized neutrons are scattered by a sample. Arrays of He-3 tubes are used to detect the position and detection timing of the scattered neutrons. The energy of the scattered neutron is calculated with the neutron TOF method. The spectrometer is designed to conduct inelastic neutron scattering experiments between cold and sub-thermal neutron energies. The details of the spectrometer are written in Ref. [5].

The graphite samples are placed in an aluminum cell and set in a refrigerator installed at the sample position of AMATERAS. The temperature was controlled at 300 K. For the ET-34 samples, 100 and 485 K measurements were also performed. Ten incident neutron energies were selected from 1.2 to 94 meV. A blank cell measurement without a graphite sample was performed to determine the background. A Vanadium sample was measured for normalization. Because Vanadium has a large incoherent cross section compared to the coherent cross section, neutrons are scattered almost isotropically. Detector efficiencies were obtained using the result of the Vanadium measurements and incoherent cross section of 5.08 b (NIST) [6].

3.2 Data analysis and results

In the analysis, after subtraction of the background deduced with the blank cell measurements, the preliminary DDSCS of each sample was derived using the detector efficiencies obtained using the Vanadium measurements. The preliminary DDSCS of the ET-34 sample at the incident neutron energy of 41.98 meV is shown in Fig. 1. Uncertainty analysis is ongoing. The DDSCS was bundled into 6 parts from 5 - 20 degree to 100 - 115 degree.

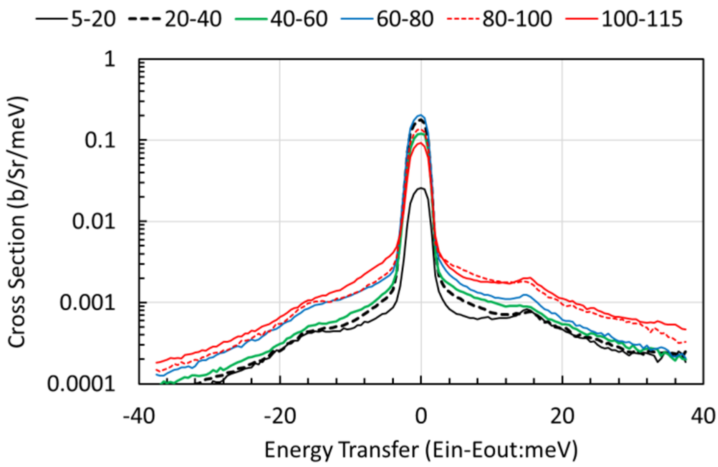

Fig. 1 The preliminary DDSCS of the ET-34 sample at incident neutron energy of 41.98 meV and temperature of 300 K.

Temperature dependences of the DDSCS of the ET-34 sample from 20 to 40 degree and from 60 to 80 degree are shown in **Fig. 2**. With decreasing the temperature, the inelastic scattering cross section decreases. The cross sections on the up-scattering side are much more degreasing than those on the slowing-down side. These are reasonable results.

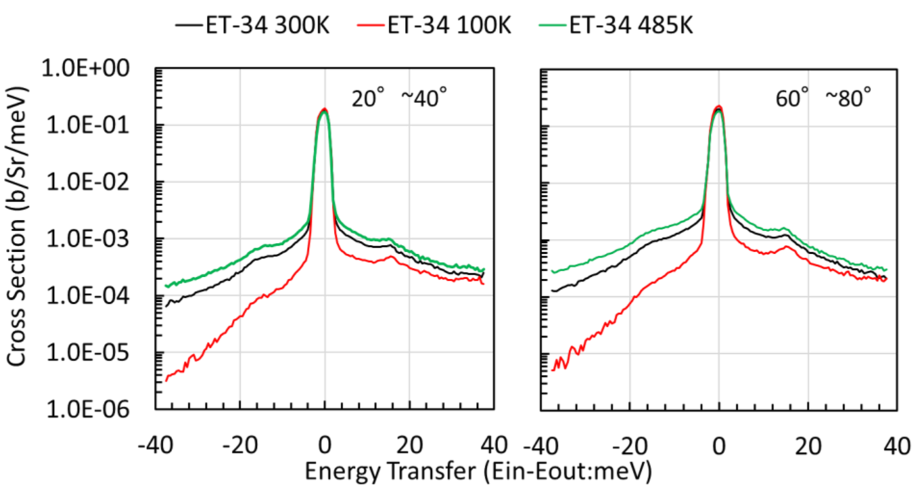

Fig. 2 Temperature dependences of the DDSCS of the ET-34 sample from 20 to 40 degree (Left) and from 60 to 80 degree (Right) at the incident neutron energy of 41.98 meV.

Sample dependences of the DDSCS are shown in Fig. 3. There’s no clear difference between the samples. The difference is less than 10 %. No porosity dependence is found in the results.

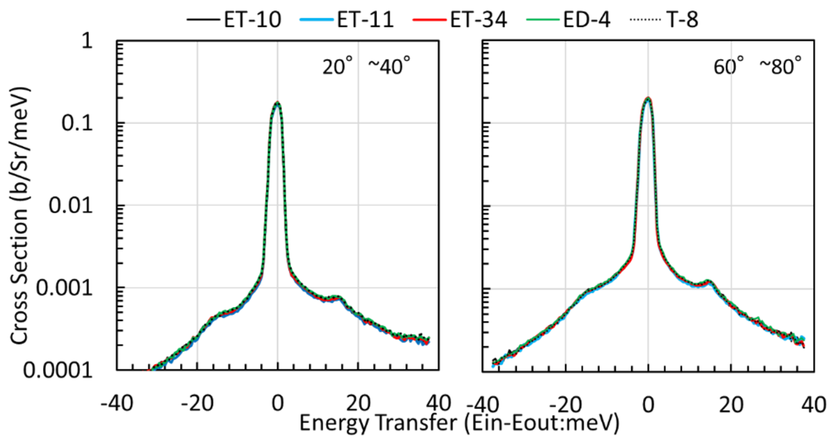

Fig. 3 Sample dependences of the DDSCS from 20 to 40 degree (Left) and from 60 to 80 degree (Right) at the incident neutron energy of 41.98 meV.

Angular dependence of the elastic cross section of each sample at the incident neutron energy of 7.74 meV is shown in Fig. 4. In elastic scattering, significant Small ANgle Scattering (SANS) and Bragg edges were observed in the derived cross sections. There is a tendency for the shape of the Bragg edge to become broader as the grain size decreases.

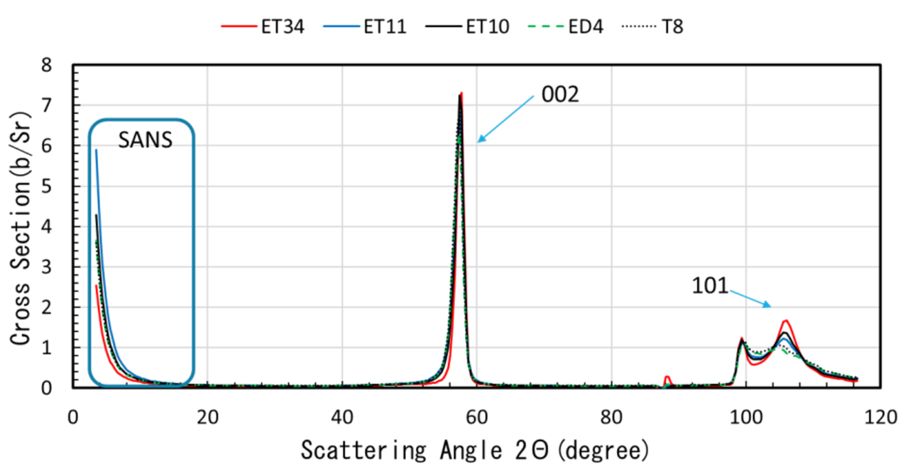

Fig. 4 Angular dependences of the elastic cross section at the incident neutron energy of 7.74 meV.

4 Total cross section measurement

4.1 Experimental setup

Neutron total cross-section measurements were performed in beamline No. 04 named Accurate Neutron-Nucleus Reaction measurement Instrument (ANNRI) with two types of Li-glass detectors installed at a flight length of 28.5 m. To determine neutron transmission spectra, a ^{6}Li-glass detector (Saint-Gobain GS-20) is utilized. This detector uses enriched

^{6}Li (>95%) and has dimensions of 50 mm x 50 mm x 1 mm for neutron detection via the ^{6}Li(n,α)^{3}H reaction. To estimate the gamma-ray background, a ^{7}Li-glass detector is used. The scintillator in the 7Li-glass detector is composed of 99.99% enriched 7Li and has a size and chemical composition similar to that of the GS-20 scintillator.

The isotropic graphite samples were placed at a flight length of 25 m. Each sample was measured for a duration of 12-16 hours, and a sample-free measurement was conducted to estimate the "sample out" condition. Transmission ratios of the neutron yields with the samples to the “sample out” were calculated, and the total cross sections were derived from the ratios. The details of the experimental setup and analysis methods are written in Refs. [7] and [8].

4.2 Data analysis and results

J-PARC was operated at a repetition rate of 25 Hz and a proton beam power of 800 kW. During the experiment, every 5.2 seconds (130 shots), the first 126 shots were delivered to the MLF, and the other 4 shots were supplied to the 50-GeV synchrotron for high-energy experiments. This allows for a 200 ms wide range TOF experiment every 5.2 seconds, which we utilized for the total cross-section measurement.

The TOF spectrum of each sample with dead time correction and γ-ray background subtraction is shown in Fig. 5. The dead-time correction was applied to the TOF spectra using the fixed dead time model, and the TOF spectra obtained using the ^{7}Li-glass detector were used to determine the observed background events due to gamma rays. In ANNRI, the trigger is generated from the previous neutron pulse with a delay of 40 ms. Therefore, the first shot to MLF is observed in the TOF region after 160 ms because there is no previous neutron pulse.

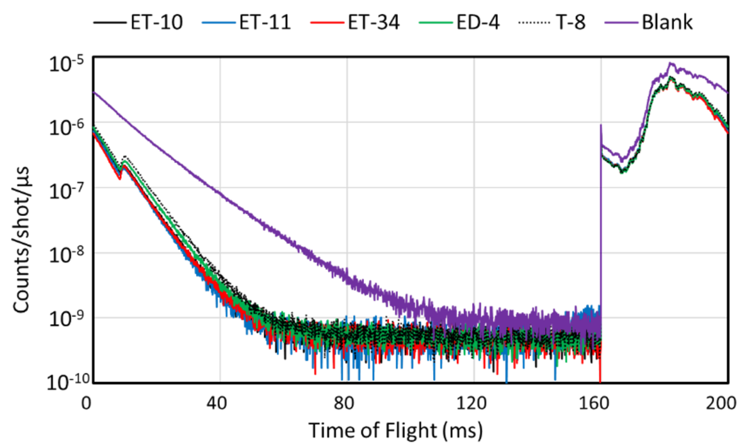

Fig. 5 TOF spectra with dead time correction and γ-ray background subtraction.

In the TOF range before 120 ms, the data after 40 ms was used as frame overlap and constant background. After 160 ms, the exponential + constant function was applied to deduce the background. The function parameters were obtained by fitting the spectra in the TOF range from 120 ms to 160 ms. Transmission ratios were calculated after subtracting the frame overlap and constant background, and the total cross sections were derived from the ratios.

The preliminary neutron total cross sections of the five isotropic graphite samples were deduced in the energy region from 1meV to 1 eV. The deduced preliminary cross sections are shown in Fig. 6 with comparison to the total cross section from ENDF/B-VIII.0

(porosity 10%). In the epithermal range (over 40 meV), all samples tended to have similar values, close to the free atom cross-section of graphite. However, at the first Bragg edge, the deduced total cross sections by those samples started to vary. The difference below 10 meV is considered to be the influence of SANS. The SANS of the isotropic graphite samples are very large compared to the traditional nuclear-grade graphite reported by Petriw et al.[2]. This is due to the uniformity of the grain size in the isotropic graphite. However, fortunately, the SANS has very little impact on criticality calculations. This is because neutron energy is not changed (SANS is elastic scattering), and only the angle is slightly changed.

In this experimental setup, scattered neutrons with angles of less than 0.25° are transmitted. However, correction of this influence was not applied in the preliminary results. The detailed analysis for this correction and uncertainties are ongoing.

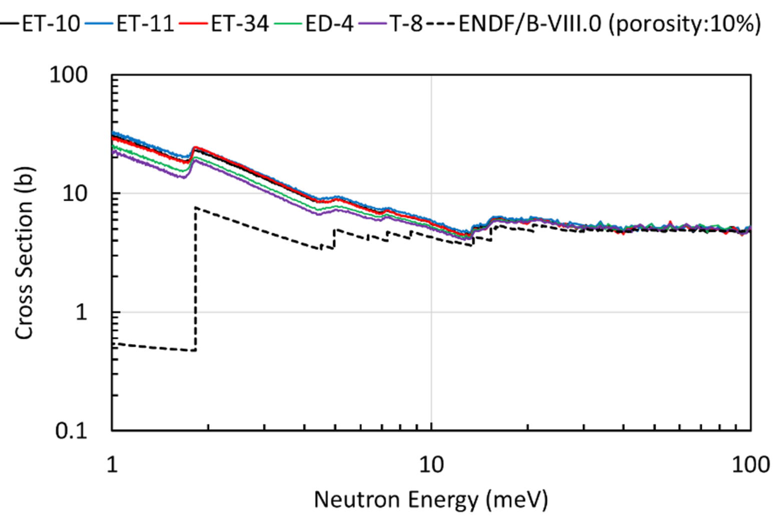

Fig. 6 The preliminary neutron total cross sections of the five isotropic graphite samples with comparison to the total cross section from ENDF/B-VIII.0 (porosity 10%).

5 Summary and outlook

The total cross-section and DDSCS of isotropic graphite have been measured in the J-PARC Materials and Life Science Experimental Facility using five samples with different porosities and grain sizes.

The DDSCS measurements were performed in Beam Line No.14 (AMATERAS) with nine incident neutron energies ranging from 1.2 to 94 meV. There is no porosity dependence in the results.

The preliminary neutron total cross sections in the energy region from 1 meV to 1 eV were deduced using Beam Line No. 04 (ANNRI). In the epithermal range (over 40 meV), all samples tended to have values close to the free atom cross-section of graphite. However, at the first Bragg edge, the deduced total cross sections by those samples started to separate from each other. The difference became more significant with decreasing the neutron energy.

In both experiments, detailed analysis for uncertainties and some corrections are ongoing.

Acknowledgment

The present study includes the result of the 'Development of Nuclear Data Evaluation Framework for Innovative Reactor' founded by the Ministry of Education, Culture, Sports, Science and Technology of Japan.

The neutron experiments at the MLF of the J-PARC were performed under the user programs (Proposal No. 2022B0109, 2022P0301, and 2023P0301).

References

1. D. Hartanto and P. H. Liem, Ann. Nucl. Energy **151**, 107943 (2021).
2. S. Petriw, J. Dawidowski, and J. Santisteban, J. Nucl. Mater. **396**, 181-188 (2010).
3. Jun Tojo, TANSO **2008,** 234, (2008) (in Japanese).
4. T. Nishihara, et al., Excellent Features of Japanese HTGR Technologies, JAEA-Technology 2018-004, 2018.
5. Nakajima, et al., J. Phys. Soc. Jpn. **80**, SB028 (2011).
6. Varley F. Sears, et al., Neutron News **3**, 29-37 (1992)
7. A. Kimura, et al., J. Nucl. Sci. Tech. **56**, 479-492 (2019).
8. A. Kimura, et al., J. Nucl. Sci. Tech. **60**, 678-696 (2023).